ISSN 0020-1685, Inorganic Materials, 2022, Vol. 58, No. 2, pp. 117–123. © Pleiades Publishing, Ltd., 2022.
Russian Text © The Author(s), 2022, published in Neorganicheskie Materialy, 2022, Vol. 58, No. 2, pp. 125–131.

Structural and Phase Transformations in the Thiourea/Zinc Acetate System

E. B. Chubenko[a, *], A. V. Baglov[a], A. A. Gnit'ko[a], S. E. Maksimov[a], V. E. Borisenko[a, b], A. I. Kulak[c], and S. V. Zlotskii[d]

[a] *Belarussian State University of Informatics and Radio Engineering, Minsk, 220013 Belarus*
[b] *Moscow Engineering Physics Institute (National Nuclear Research University), Moscow, 115409 Russia*
[c] *Institute of General and Inorganic Chemistry, Belarussian Academy of Sciences, Minsk, 220072 Belarus*
[d] *Belarussian State University, Minsk, 220030 Belarus*
**e-mail: eugene.chubenko@gmail.com*

Received June 28, 2021; revised November 17, 2021; accepted November 18, 2021

Abstract—Using differential thermal analysis and thermogravimetry, we have studied thermal decomposition of a mechanical mixture of thiourea and zinc acetate, resulting in the formation of a composite material consisting of graphitic carbon nitride and zinc acetate, g-C_3N_4/ZnS, and possibly containing zinc oxide (ZnO) inclusions. In the case of a mixture containing the stoichiometric sulfur : zinc ratio for zinc sulfide synthesis, one can obtain a material containing only ZnS semiconductor crystals embedded in a g-C_3N_4 matrix. ZnS is formed in the temperature range 317–367°C as a result of decomposition of zinc complexes with thiourea. Heating the mixture to above 560°C increases the rate of the thermal decomposition of g-C_3N_4, which reaches completion between 720 and 740°C. The presence of oxygen in the reaction atmosphere also accelerates this process, without significantly changing the temperature range of synthesis or decomposition of reaction products. The proposed technique can be used for the synthesis of g-C_3N_4-based composite materials and other semiconducting metal sulfides.

Keywords: graphitic carbon nitride, zinc sulfide, differential thermal analysis, thermogravimetry, X-ray diffractometry

DOI: 10.1134/S0020168522020054

INTRODUCTION

Zinc sulfide (ZnS) and zinc oxide (ZnO) are wide-band-gap semiconductors with band gap $E_{g\,ZnS}$ = 3.6 eV and $E_{g\,ZnO}$ = 3.36 eV at 300 K, respectively. The direct energy bands in these materials ensure efficient room-temperature ultraviolet luminescence, attractive for a number of practical applications. ZnS and ZnO can be used in gas sensors, photocatalytic coatings, solar cells, and piezoelectric energy nanogenerators [1–5]; as luminescent materials; and in light-emitting diodes and lasers [6, 7]. ZnS single crystals doped with silver ions are used as scintillators for ionizing radiation detection [8]. ZnO and ZnS nanoparticles are used in semiconductor quantum dot light-emitting diode displays [9].

Graphitic carbon nitride (g-C_3N_4) is also a semiconductor ($E_g \approx 2.7$ eV at 300 K) and has a graphite-like layered structure in which each layer is made up of cells similar to heptazine molecules [10]. g-C_3N_4 has attracted considerable interest owing to its excellent photocatalytic and photoluminescent properties, attractive for practical application [11]. Moreover, it is easy to synthesize via heat treatment of nitrogen-rich organic compounds, for example, melamine [12], cyanamides [13, 14], urea, and thiourea [15].

Composites of g-C_3N_4 and ZnS have been reported in the literature and can be prepared by a variety of techniques [16]. Such materials ensure improved separation of photogenerated electron–hole pairs, which allows them to bring about effective photocatalysis in the visible spectral region. A typical process for the fabrication of such composites involves separate syntheses and subsequent intermixing of their components.

Previously, Chubenko et al. [17] proposed a method for one-step synthesis of g-C_3N_4-based composites via pyrolytic decomposition of a mechanical mixture of thiourea and zinc acetate, which significantly simplified and accelerated the synthesis process in comparison with multistep methods [11].

The purpose of this work was to study in detail the phase transformations in the thiourea–zinc acetate system in the temperature range 500–625°C by differential thermal analysis and thermogravimetry with the aim of developing processes for the fabrication of

g-C_3N_4-based composites with tailored composition and properties.

EXPERIMENTAL

Composite materials were synthesized in a 20 cm^3 ceramic crucible mechanically sealed so as to ensure free outflow of gaseous reaction products from the crucible during decomposition of the starting materials and simultaneously limit air inflow. Thus, the synthesis conditions can be thought of as quasi-gas-tight. The atmosphere in the crucible consisted of air containing oxygen and water vapor. In the crucible we placed a mixture of mechanically comminuted thiourea ($CS(NH_2)_2$) and zinc acetate dihydrate ($Zn(O_2CCH_3)_2{\cdot}2H_2O$). Two compositions were used: stoichiometric composition for ZnS synthesis—25.75 wt % $CS(NH_2)_2$ + 74.25 wt % $Zn(O_2CCH_3)_2{\cdot}2H_2O$—and composition for the preparation of a g-C_3N_4/ZnS composite—90 wt % $CS(NH_2)_2$ + 10 wt % $Zn(O_2CCH_3)_2{\cdot}2H_2O$. In both cases, the total weight of the chemical compounds loaded into the crucible was 2 g. Heat treatment was carried out in a muffle furnace for 30 min at temperatures from 500 to 625°C. The average heating rate was 12°C/min. After heat treatment, the synthesis products were furnace-cooled to room temperature.

The morphology of the resultant materials was examined by scanning electron microscopy (SEM) on a Hitachi S-4200 microscope. Their crystal structure and phase composition were determined by X-ray diffraction on a DRON-4 diffractometer with CuK_α radiation (λ = 0.154184 nm). Structural and phase transformations were investigated by differential thermal analysis (DTA), thermogravimetry (TG), and derivative thermogravimetry (DTG) using a Netzsch STA 409 PC/PG system. Data were collected in the range 25–800°C at a heating rate of 10°C/min in an argon atmosphere or argon–air mixture with an argon : air volume ratio of 1 : 1.

RESULTS AND DISCUSSION

The X-ray diffraction data in Fig. 1 confirm that heat treatment of $CS(NH_2)_2$ in the temperature range 450–625°C led to the formation of pyrolytic g-C_3N_4

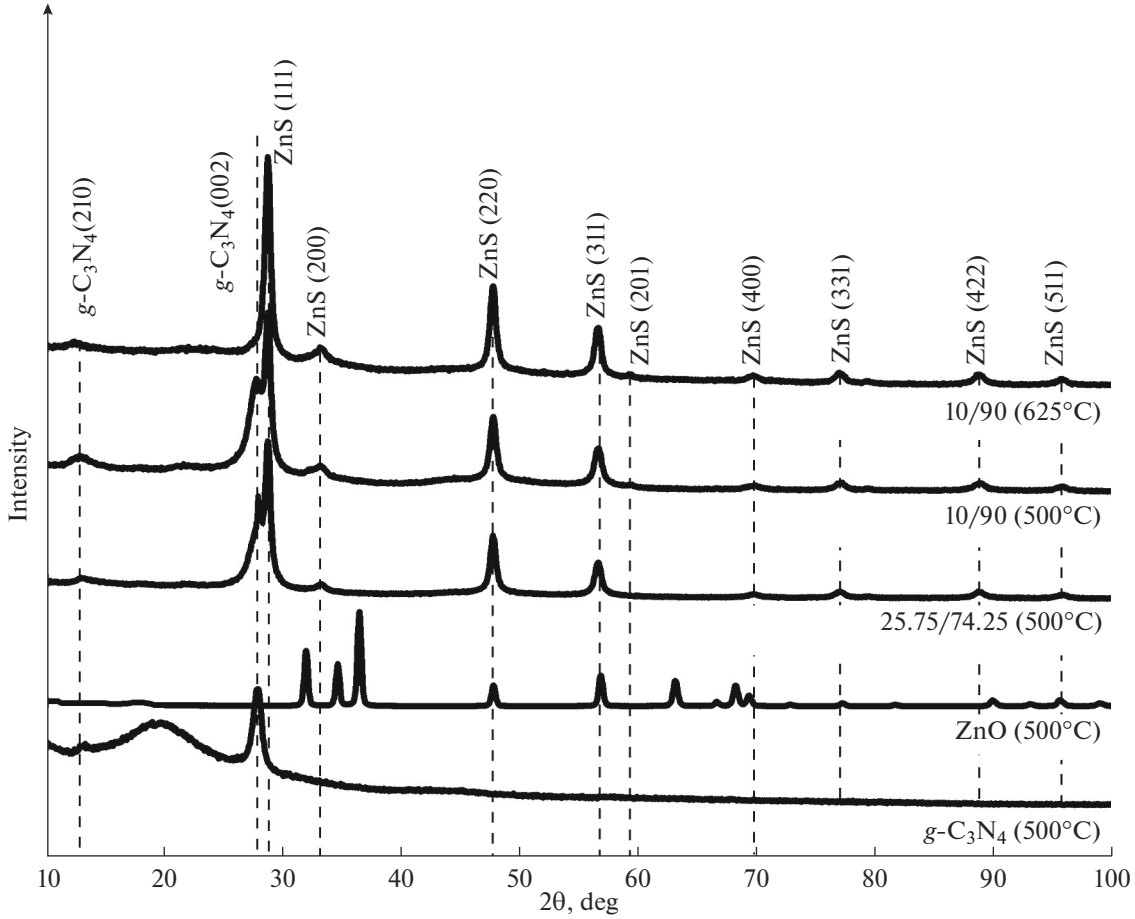

Fig. 1. X-ray diffraction patterns of ZnS synthesized via thermal decomposition of $Zn(O_2CCH_3)_2{\cdot}2H_2O$, g-C_3N_4 prepared via thermal decomposition of $CS(NH_2)_2$, and composites prepared from a 25.75 wt % $CS(NH_2)_2$ + 74.25 wt % $Zn(O_2CCH_3)_2{\cdot}2H_2O$ mixture at 500°C and from a 90 wt % $CS(NH_2)_2$ + 10 wt % $Zn(O_2CCH_3)_2{\cdot}2H_2O$ mixture at 500 and 625°C.

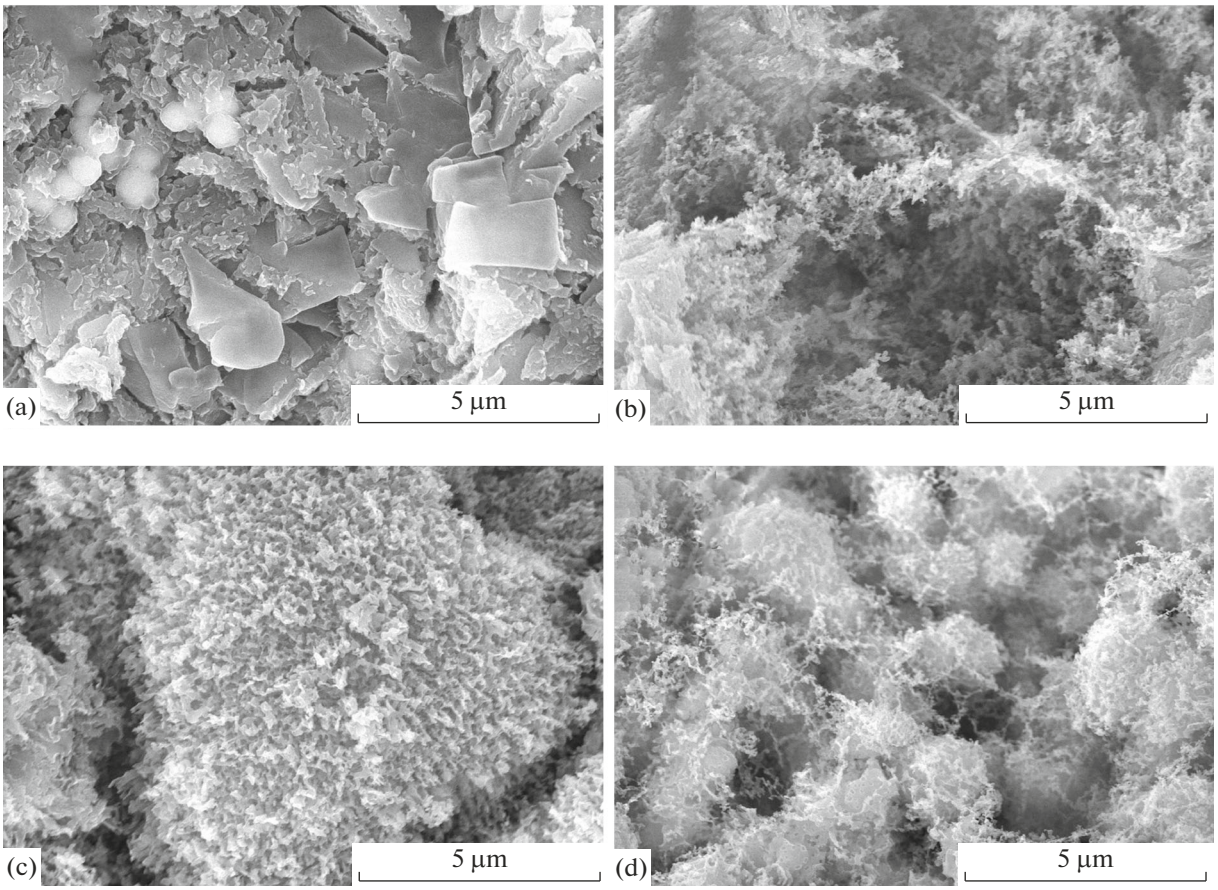

Fig. 2. Microstructure of the composites synthesized at (a) 550, (b) 575, (c) 600, and (d) 625°C from a 90 wt % $CS(NH_2)_2$ + 10 wt % $Zn(O_2CCH_3)_2 \cdot 2H_2O$ mixture.

and that heat treatment of $Zn(O_2CCH_3)_2 \cdot 2H_2O$ in this temperature range yielded crystalline ZnO, in agreement with previously reported results [18, 19]. Heat treatment of the stoichiometric mixture of the starting materials, containing 25.75 wt % $CS(NH_2)_2$ and 74.25 wt % $Zn(O_2CCH_3)_2 \cdot 2H_2O$, allowed us to obtain a composite consisting of *g*-C_3N_4 and ZnS with a cubic (sphalerite) structure, as was evidenced by the set of reflections characteristic of this semiconductor and observed in its X-ray diffraction pattern (Fig. 1). Heat treatment of the thiourea-rich mixture of the starting materials, consisting of 90 wt % $CS(NH_2)_2$ and 10 wt % $Zn(O_2CCH_3)_2 \cdot 2H_2O$, in the temperature range indicated above led to the formation of a composite consisting of both *g*-C_3N_4 and ZnS, possibly with ZnO as an impurity phase (Fig. 1). The presence of the oxide was suggested by only one, relatively weak reflection, at $2\theta = 69°$. Most reflections from ZnO with a hexagonal (wurtzite) structure are not seen in X-ray diffraction patterns. The possibility of the existence of a crystalline ZnO phase in composites prepared by the method in question was inferred previously [17, 20] from the presence of a photoluminescence band characteristic of ZnO and related to lattice defects. ZnO formation can be due to the interaction of Zn atoms with the water vapor resulting from $Zn(O_2CCH_3)_2 \cdot 2H_2O$ dehydration and decomposition, and remaining in the crucible throughout the synthesis process, and with atmospheric oxygen present in the crucible. The excess of thiourea in the starting mixture can block water vapor release from molten $Zn(O_2CCH_3)_2$, creating favorable conditions for ZnO formation. The oxide is a more stable compound than is ZnS, so it undergoes no sulfidation as the temperature is raised or in the presence of excess sulfur in the reaction zone. The absence of the 002 reflection from *g*-C_3N_4 after synthesis at a temperature of 625°C is due to delamination of this compound because the van der Waals bonds that keep together individual layers of the material rupture at temperatures above 600°C [11]. At the same time, *g*-C_3N_4 does not undergo complete decomposition in this process, as evidenced by the fact that the 210 peak of *g*-C_3N_4 persists in X-ray diffraction patterns.

Heat treatment of a mixture of the starting materials at 550°C led to the formation of a composite consisting of particles less than 500 nm in size, platelike inclusions ranging in size from 2 to 3 μm, and spherical particles about 800 nm in diameter (Fig. 2a). Given that *g*-C_3N_4 crystals resulting from thiourea decompo-

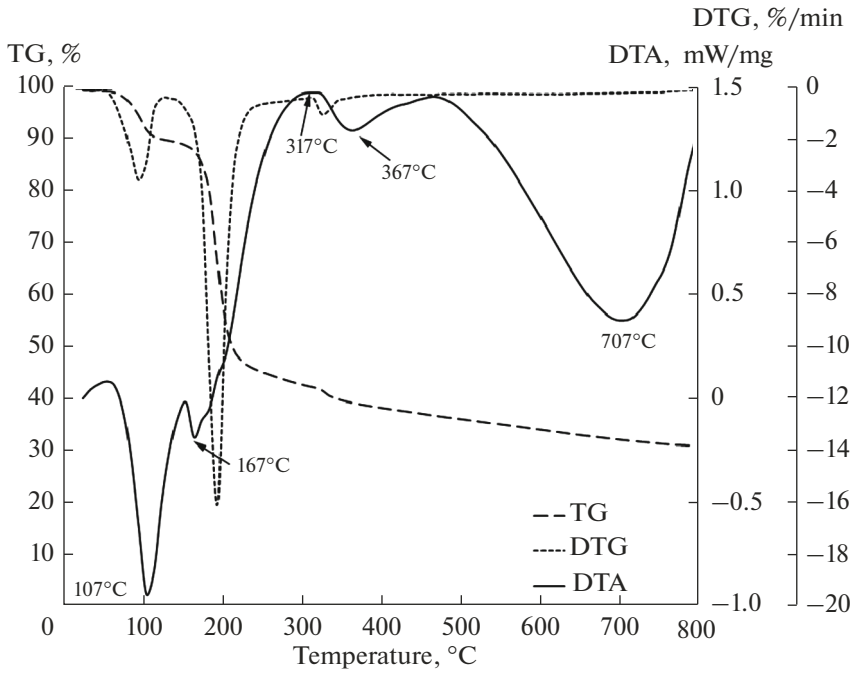

Fig. 3. TG, DTA, and DTG curves of a 25.75 wt % $CS(NH_2)_2$ + 74.25 wt % $Zn(O_2CCH_3)_2 \cdot 2H_2O$ stoichiometric mixture for ZnS synthesis in an argon atmosphere.

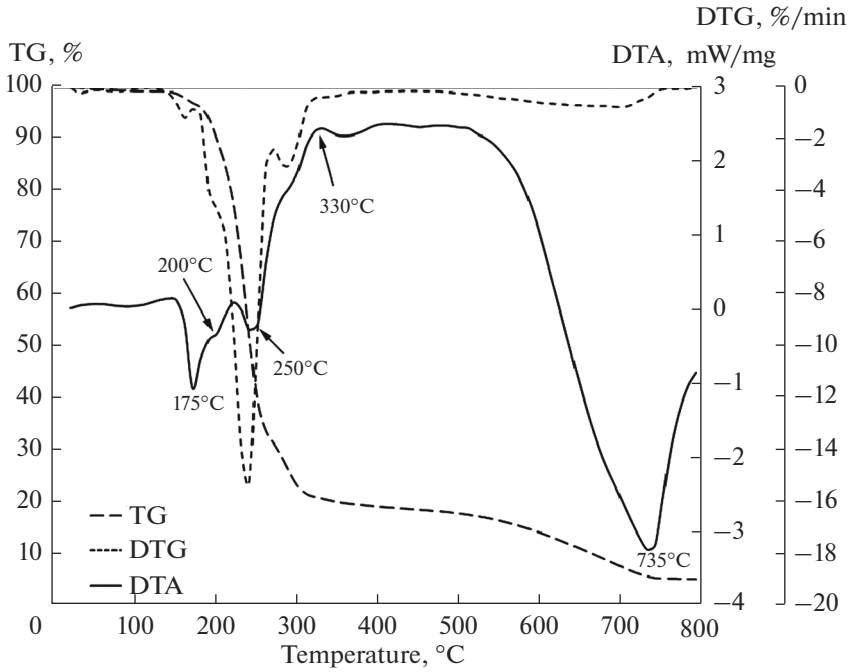

Fig. 4. TG, DTA, and DTG curves of a 90 wt % $CS(NH_2)_2$ + 10 wt % $Zn(O_2CCH_3)_2 \cdot 2H_2O$ thiourea-rich mixture in an argon atmosphere.

sition are usually platelike in shape [19], it is reasonable to assume that the spherical particles in the composite we produced consist of ZnS and that the platelike particles consist of g-C_3N_4, whereas submicron fragments result from thermal defoliation of larger plates. The particle size of g-C_3N_4 further decreases as the temperature is raised from 550 to 625°C (Fig. 2). It is well seen that the microstructure of the composite includes a porous g-C_3N_4 shell covering dense ZnS particles. With increasing temperature, the porosity of

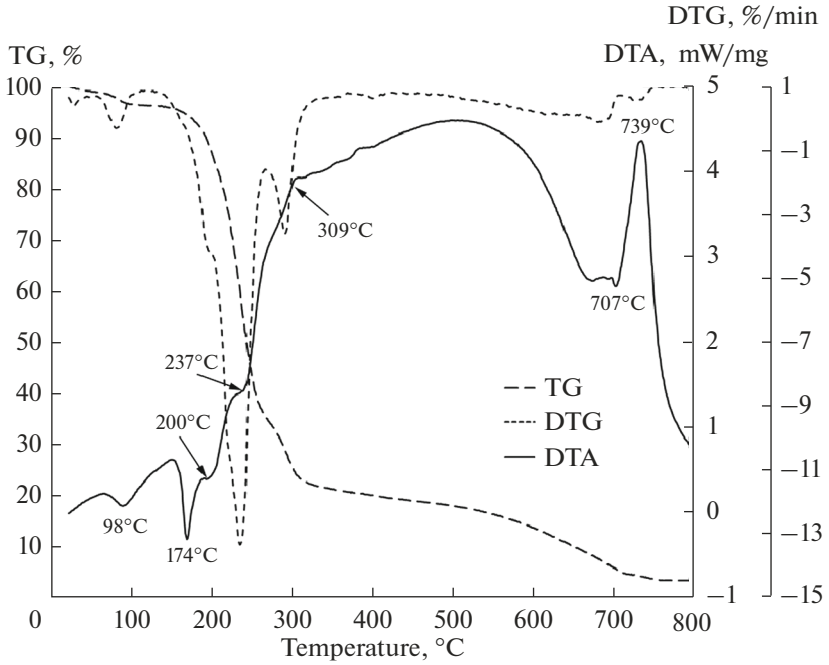

Fig. 5. TG, DTA, and DTG curves of a 90 wt % $CS(NH_2)_2$ + 10 wt % $Zn(O_2CCH_3)_2{\cdot}2H_2O$ thiourea-rich mixture in an argon–air atmosphere.

the shell increases as a result of g-C_3N_4 decomposition at temperatures above 575°C. The shell consists of platelets on the order of 25 nm in thickness and 50 to 100 nm in side length, which form a network of cells ranging in size from 300 to 500 nm.

The DTA, TG, and DTG results for the starting mixture with the stoichiometric composition for ZnS synthesis (Fig. 3) demonstrate that, in the range 107–167°C, zinc acetate melts and dissolves thiourea to form a zinc complex with thiourea, $[Zn(CS(NH_2)_2)_2{\cdot}(CH_3COO)_2]$, which then decomposes at temperatures from 317 to 367°C to form ZnS with a hexagonal structure. At 707°C, it probably undergoes a phase transition to cubic ZnS.

The thermal analysis results for the 90 wt % $CS(NH_2)_2$ + 10 wt % $Zn(O_2CCH_3)_2{\cdot}2H_2O$ mixture are presented in Fig. 4. Because of the relatively low concentration of zinc acetate in the mixture, there is no peak attributable to its melting (107°C). Other typical peaks are also missing or shifted relative to values determined in the case of ZnS synthesis (Fig. 3). The polymerization of azine rings during g-C_3N_4 synthesis is known to occur in the range 250–330°C, overlapping with the ZnS formation process between 317 and 367°C. In addition, raising the temperature leads to g-C_3N_4 decomposition, which accelerates starting at 560°C and reaches completion between 730 and 740°C.

Since the composite was synthesized in a quasi-gas-tight crucible under an atmosphere containing oxygen and water vapor, it is reasonable to compare the thermal analysis data considered above with analogous data obtained under an argon–oxygen atmosphere. The corresponding data presented in Fig. 5 demonstrate that the presence of oxygen has a significant effect on the processes in the composite system, primarily accelerating g-C_3N_4 decomposition. In addition, there is a peak at a temperature of 707°C, due to the phase transition of ZnS.

CONCLUSIONS

Heat treatment of a 25.75 wt % $CS(NH_2)_2$ + 74.25 wt % $Zn(O_2CCH_3)_2{\cdot}2H_2O$ mixture in the temperature range 500–625°C leads to the formation of a composite material consisting of ZnS particles on the order of 800 nm in size in a g-C_3N_4 matrix. Raising the temperature from 575 to 625°C leads to defoliation of large g-C_3N_4 plates, about 2–3 μm in size, into smaller plates, less than 100 nm in size, which form a porous structure coating the ZnS particles.

The use of DTA, TG, and DTG for gaining insight into phase transformations in the thiourea–zinc acetate system has made it possible to find that ZnS synthesis proceeds through the formation of zinc complexes with thiourea at temperatures from 107 to 167°C, followed by their decomposition in the range 317–367°C and the formation of ZnS with hexagonal symmetry. Further raising the temperature leads to g-C_3N_4 decomposition. The process speeds up starting at a temperature of 560°C and reaches completion between 720 and 740°C. The presence of oxygen also accelerates this process, without significantly chang-

ing the temperature range of synthesis or decomposition of reaction products.

The composite material obtained in the case of a starting mixture with a nonstoichiometric composition relative to ZnS, 10 wt % $CS(NH_2)_2$ + 90 wt % $Zn(O_2CCH_3)_2{\cdot}2H_2O$, possibly contains the ZnO phase.

Thus, we have proposed a simple, one-step technique for the synthesis of nanostructured composites by heating a starting mixture containing a metal acetate and thiourea in a closed crucible. The use of thiourea allows one to synthesize metal sulfides through the formation of a complex of metal ions with thiourea, and a considerable excess of thiourea in a starting mixture helps obtain a nanostructured g-C_3N_4 matrix for the sulfides being synthesized.

The proposed technique can be useful for the synthesis of nanostructured composites containing fillers in the form of narrow-band-gap semiconducting metal sulfides, including those with properties of topological insulators, and their combinations.

ACKNOWLEDGMENTS

We are grateful to V.V. Uglov and D.V. Zhigulin for characterizing the experimental samples by X-ray diffraction and scanning electron microscopy, respectively.

FUNDING

This work was supported by the Ministry of Education of the Republic of Belarus through the Materials Research, Novel Materials, and Advanced Technologies National Research Program (task no. 1.4) and the Photonics and Electronics for Innovations National Research Program (task no. 2.2).

V. E. Borisenko acknowledges the partial support from the Russian Federation Ministry of Science and Higher Education through the program aimed at improving the competitiveness of the Moscow Engineering Physics Institute (National Nuclear Research University).

CONFLICT OF INTEREST

The authors declare that they have no conflicts of interest.

REFERENCES

1. Peshkova, T.V., Dimitrov, D.Ts., Nalimova, S.S., Kononova, I.E., Nikolaev, N.K., Papazova, K.I., Bozhinova, A.S., Moshnikov, V.A., and Terukov, E.I., Structures of nanowires with Zn–ZnO:CuO junctions for detecting ethanol vapors, *Tech. Phys.,* 2014, vol. 59, pp. 771–776. https://doi.org/10.1134/S1063784214050259
2. Bozhinova, A.S., Kaneva, N.V., Kononova, I.E., Nalimova, S.S., Syuleiman, Sh.A., Papazova, K.I., Dimitrov, D.Ts., Moshnikov, V.A., and Terukov, E.I., Study of the photocatalytic and sensor properties of ZnO/SiO_2 nanocomposite layers, *Semiconductors,* 2013, vol. 47, pp. 1636–1640. https://doi.org/10.1134/S106378261312004X
3. Pronin, I.A., Kaneva, N.V., Bozhinova, A.S., Averin, I.A., Papazova, K.I., Dimitrov, D.Ts., and Moshnikov, V.A., Photocatalytic oxidation of pharmaceuticals on thin nanostructured zinc oxide films, *Kinet. Catal.,* 2014, vol. 55, pp. 166–170. https://doi.org/10.1134/10.1134/S0023158414020074
4. Law, M., Greene, L.E., Johnson, J.C., Saykally, R., and Yang, P.D., Nanowire dye-sensitized solar cells, *Nat. Mater.,* 2005, vol. 4, pp. 455–459. https://doi.org/10.1038/nmat1387
5. Wang, Z.L. and Song, J.H., Piezoelectric nanogenerators based on zinc oxide nanowire arrays, *Science,* 2006, vol. 312, pp. 242–246. https://doi.org/10.1126/science.1124005
6. Park, W.I. and Yi, G.C., Electroluminescence in *n*-ZnO nanorod arrays vertically grown on *p*-GaN, *Adv. Mater.,* 2004, vol. 16, pp. 87–90. https://doi.org/10.1002/adma.200305729
7. Govender, K., Boyle, D.S.O., Brien, P., Binks, D., West, D., and Coleman, D., Room-temperature lasing observed from ZnO nanocolumns grown by aqueous solution deposition, *Adv. Mater.,* 2002, vol. 14, pp. 1221–224. https://doi.org/10.1002/chin.200247008
8. Rodnyi, P.A., Gorohova, E.I., Mikhrin, S.B., Mishin, A.N., and Potapov, A.S., Quest and investigation of long wavelength scintillators, *Nucl. Instrum. Methods Phys. Res., Sect. A,* 2002, vol. 486, pp. 244–249. https://doi.org/10.1016/S0168-9002(02)00710-6
9. Qian, L., Zheng, Y., Jiangeng, X., and Holloway, P.H., Stable and efficient quantum-dot light-emitting diodes based on solution-processed multilayer structures, *Nat. Photonics,* 2011, vol. 5, pp. 543–548. https://doi.org/10.1038/nphoton.2011.171
10. Chu, S., Wang, Y., Guo, Y., Feng, J., Wang, C., Luo, W., Fan, X., and Zou, Z., Band structure engineering of carbon nitride: in search of a polymer photocatalyst with high photooxidation property, *ACS Catal.,* 2013, vol. 3, pp. 912–919. https://doi.org/10.1021/cs4000624
11. Thomas, A., Fischer, A., Goettmann, F., Antonietti, M., Müller, J.-O., Schlögl, R., and Carlsson, J.M., Graphitic carbon nitride materials: variation of structure and morphology and their use as metal-free catalysts, *J. Mater. Chem.,* 2008, vol. 18, pp. 4893–4908. https://doi.org/10.1039/B800274F
12. Chubenko, E.B., Baglov, A.V., Lisimova, E.S., and Borisenko, V.E., Synthesis of graphitic carbon nitride in porous silica glass, *Int. J. Nanosci.,* 2019, vol. 18, paper 1940042. https://doi.org/10.1142/S0219581X19400428
13. Yuan, J., Liu, X., Tang, Y., Zeng, Y., Wang, L., Zhang, S., Cai, T., Liu, Y., Luo, S., Pei, Y., and Liu, C., Positioning cyanamide defects in g-C_3N_4: engineering energy levels and active sites for superior photocatalytic hydrogen evolution, *Appl. Catal., B,* 2018, vol. 237, pp. 24–31. https://doi.org/10.1016/j.apcatb.2018.05.064
14. Zhang, M., Xu, J., Zong, R., and Zhu, Y., Enhancement of visible light photocatalytic activities via porous

structure of g-C_3N_4, *Appl. Catal., B,* 2014, vol. 147, pp. 229–235.
https://doi.org/10.1016/j.apcatb.2013.09.002

15. Dong, F., Zhao, Z., Xiong, T., Ni, Z., Zhang, W., Sun, Y., and Ho, W.-K., In situ construction of g-C_3N_4/g-C_3N_4 metal-free heterojunction for enhanced visible-light photocatalysis, *ACS Appl. Mater. Interfaces,* 2013, vol. 5, pp. 11392–11401.
https://doi.org/10.1021/am403653a

16. Hao, X., Zhou, J., Cui, Z., Wang, Y., Wang, Y., and Zou, Z., Zn-vacancy mediated electron-hole separation in ZnS/g-C_3N_4 heterojunction for efficient visible-light photocatalytic hydrogen production, *Appl. Catal., B,* 2018, vol. 229, pp. 41–51.
https://doi.org/10.1016/j.apcatb.2018.02.006

17. Chubenko, E.B., Baglov, A.V., and Borisenko, V.E., One-step synthesis of visible range luminescent multicomponent semiconductor composites based on graphitic carbon nitride, *Adv. Photonics Res.,* 2020, vol. 1, paper 2000004.
https://doi.org/10.1002/adpr.202000004

18. Baglov, A.V., Chubenko, E.B., Hnitsko, A.A., Borisenko, V.E., Malashevich, A.A., and Uglov, V.V., Structural and photoluminescence properties of graphite-like carbon nitride, *Semiconductors,* 2020, vol. 54, pp. 228–232.
https://doi.org/10.1134/S1063782620020049

19. Silva, T.G., Silveira, E., Ribeiro, E., Machado, K.D., Mattoso, N., and Hümmelgen, I.A., Structural and optical properties of ZnO films produced by a modified ultrasonic spray pyrolysis technique, *Thin Solid Films,* 2014, vol. 551, pp. 13–18.
https://doi.org/10.1016/j.tsf.2013.11.011

20. Chubenko, E.B., Baglov, A.V., Leanenia, M.S., Urmanov, B.D., and Borisenko, V.E., Broad band photoluminescence of g-C_3N_4/ZnO/ZnS composite towards white light source, *Mater. Sci. Eng., B.,* 2021, vol. 267, paper 115109.
https://doi.org/10.1016/j.mseb.2021.115109